# CHAPTER IV
## PREPARATION AND ADSORTION BEHAVIOR OF AMINATED ELECTROSPUN POLYACRYLONITRILE NANOFIBER MATS FOR HEAVY METAL ION REMOVAL

## 4.1 Abstract

A polyacrylonitrile (PAN) nanofiber mat was prepared by electrospinning and it was further modified to contain amidino diethylenediamine chelating groups on their surface via heterogeneous reaction with diethylenetriamine (DETA). The obtained aminated PAN (APAN) nanofiber mats were evaluated for their chelating property with four types of metal ions, namely Cu(II), Ag(I), Fe(II), and Pb(II) ions. The amounts of the metal ions adsorbed onto the APAN nanofiber mats were influenced by the initial pH and the initial concentration of the metal ion solutions. Increasing the contact time also resulted in a monotonous increase in the adsorbed amounts of the metal ions, which finally reached equilibrium values at about 10 h for Cu(II) ions and about 5 h for Ag(I), Fe(II), and Pb(II) ions. The maximal adsorption capacities of the metal ions on the APAN nanofiber mats, as calculated from the Langmuir model, were 150.6, 155.5, 116.5, and 60.6 $mg \cdot g^{-1}$, respectively.

(**Key-words**: electrospinning, aminated polyacrylonitrile, metal ion removal)

## 4.2 Introduction

Nowadays, pollution of water from the contamination of heavy metals is a serious environmental problem. Metals such as copper, silver, iron, lead, chromium, and zinc, which have high toxic and non-biodegradable properties, can cause problems for both the environment and the living organisms [1, 2]. Many methods (such as precipitation, electroplating, ion exchange, membrane separation, and adsorption, etc.) are being used to remove the ions of these metals from aqueous effluents [3-7]. Adsorption is commonly regarded as an effective and economical method for wastewater treatment. Various types of adsorbents [such as, activated carbons [8-10], chitosan/natural zeolites [11, 12], biosorbents [13-15], chelating materials [16, 17] have been studied for the adsorption of metal ions from aqueous solutions. The adsorption properties of these adsorbents depend on the functional group(s) on their surfaces, where it has been found that an adsorbent containing nitrogen-based ligands (such as, amino, amidoxime, imidazole, and hydrazine groups) was effective in forming complexation with metal ions [17-24].

Recently, nano-meter-sized materials are very interesting in their development as adsorbent materials, because of their high surface area to unit mass ratios. There have been a number of research work on nano-adsorbents, including nanobeads [25], nanocomposites [26], magnetic-nano adsorbents [27], and nanofiber mats [28]. Among these materials, nanofiber mats have attracted a great deal of attention because of their many advantages, such as high porosity, high gas permeability, and high specific surface area per unit mass, which should lead to a high adsorption capacity. Polyacrylonitrile (PAN) microfibers have been widely modified to contain a chelating group for metal ion removal, because it is a cheap and common commercial product. Additionally, PAN can easily be prepared into nanofiber mats by a facile fiber spinning process called electrospinning [29].

Electrospinning is a process capable of producing ultrafine fibers, with diameters as small as nano- to micro-meter range, from materials of diverse origins, including polymers [30]. In a general set-up, a polymer liquid (i.e., melt or solution) is first loaded into a container with a nozzle and then charged with a high electrical potential across a finite distance between the nozzle and a grounded collection

device. When the electric field increases beyond a critical value, a charged jet is ejected [31]. As the jet travels to the collector, it either cools down or the solvent evaporates to obtain ultrafine fibers in the form of a non-woven fabric on the collector. The morphology of the electrospun fibers depends on a number of factors, such as solution properties, processing conditions, and ambient conditions [32]. The proposed uses for these fibers are, for examples, scaffolds for tissue engineering [33] and carriers for the delivery of DNA and drugs [34, 35]. Furthermore, the introduction of appropriate functional groups onto the surface of an electrospun nanofiber mat allows it to be used as an adsorbent in waste water treatment[28]. It is therefore of our interest to investigate the feasibility of using a nanofiber mat that bears amine groups on its surface as an adsorbing substrate of metal ions.

The aim of the present contribution was to synthesize aminated PAN nanofiber mats from the reaction between electrospun PAN nanofiber mats and diethylenetriamine (DETA). Characterization of the obtained nanofiber mats was studied by Fourier-transform infrared spectroscopy (FT-IR) and scanning electron microscopy (SEM). The effects of pH, the contact time, and the initial metal ion concentration on the adsorption capacity of the APAN nanofiber mats for Cu(II), Ag(I), Fe(II), and Pb(II) ions were examined by atomic absorption spectroscopy (AAS). Desorption of the metal ions from the APAN nanofiber mats was also examined using hydrochloric acid (HCl) aqueous solutions of varying concentrations.

**4.3 Experimental Details**

4.3.1 Materials

Polyacrylonitrile (PAN) microfibers, used as the raw material for preparing PAN solutions for further electrospinning into ultrafine PAN fiber mats, were received from Thai Acrylic Fibre Co., Ltd. (Thailand). The polymer contained 91.4 wt.% acrylonitrile monomer ($CH_2$=CHCN) and 8.6 wt.% methylacrylate comonomer ($CH_2$=CHCOOHCH$_3$). The weight-average molecular weight of polymer was about 55 500 Da. Dimethylformamide (DMF; ~99.98% purity) and ethanol (analytical reagent grade) were purchased from Lab-scan Asia Co., Ltd.

(Thailand). Diethylenetriamine (DETA; ~99% purity) and aluminium chloride hexahydrate (AlCl$_3$·6H$_2$O; ~99% purity) were purchased from Sigma-Aldrich (USA). Stock solutions of metal ions were prepared from copper(II) chloride dihydrate (CuCl$_2$·2H$_2$O, ~99% purity; Sigma-Aldrich, USA), silver nitrate (AgNO$_3$, ~99.998% purity; Fisher Scientific, USA), lead(II) nitrate [Pb(NO$_3$)$_2$, ~99% purity; Ajax Finechem, Australia], and iron(II) sulphate (FeSO$_4$, ~99% purity; Ajax Finechem, Australia).

### 4.3.2 Electrospun Fibers from PAN Solution

Electrospun PAN fiber mats were prepared in a similar manner to that reported by Sutasinpromprae et al. [29]. Briefly, the solution was prepared at 10 wt.% from the as-received PAN microfibers in DMF. The as-prepared solutions were then electrospun, under a fixed electric field of 15 kV/20 cm using a Gamma High Voltage Research D-ES30PN/M692 dc power supply, onto an aluminum (Al) sheet wrapped around a rotating cylinder (width and OD of the cylinder ≈ 15 cm; rotational speed ≈50 rpm), which was used as the collector. The electrospun fiber mats were collected continuously for 48 h (resulting in the fiber mats of 125 ± 10 μm in thickness). The electrospun PAN fiber mats had been placed *in vacuo* at room temperature (25 ± 1 °C) in order to remove as much solvent from them as possible, prior to further processing.

### 4.3.3 Preparation of Aminated PAN Nanofiber Mats

Aminated PAN (hereafter, APAN) nanofiber mats were synthesized based on a procedure that was adapted from that reported by Ko et al. (24). Briefly, the electrospun PAN fiber mats (0.6 g) were placed into a sealed chamber containing 50 mL of DETA and 2.0 g of AlCl$_3$·6H$_2$O. The reaction temperature was fixed at 90 °C and the reaction time was varied from 1 to 5 h. After the reaction, the obtained fiber mats were washed successively with distilled water and ethanol, and were then dried *in vacuo* at room temperature (25 ± 1 °C). For comparison purposes, APAN fibers were also synthesized from the as-received PAN microfibers at 90 °C with the reaction time being selected from the optimal condition of the APAN nanofiber mats.

### 4.3.4 Characterization

Morphologies of both of the PAN and the APAN nanofiber mats were observed by a JEOL JSM-6400 scanning electron microscope (SEM). Each specimen was coated with a thin layer of gold using a JEOL JFC-1100E sputtering device prior to the SEM observation. The diameters of the individual fiber segments within each specimen were measured directly from the SEM images using SemAphore 4.0 software. No less than fifty diameters were determined on different fiber segments and the average value was calculated. A Thermo-Nicolet Nexus 670 Fourier-transform infrared spectroscope (FT-IR) from KBr pellets, operating at a resolution of 4 cm$^{-1}$ and a wavenumber range of 4000 to 400 cm$^{-1}$, was used to characterize the neat and the modified electrospun PAN fiber mats. The conversion of the nitrile group into the amidino diethylenediamine group ($C_n$, in %) on the surface of each of the modified PAN fiber mats was estimated as follows [28]:

$$C_n = \frac{W_1 - W_0}{W_0} \times \frac{M_0}{M_1} \times 100, \qquad (1)$$

where $W_1$ and $W_0$ (i.e., 0.6 g) are the weights of the PAN fiber mat after and before the reaction, $M_0$ is the molecular weight of the acrylonitrile monomer (i.e., 53 g.mol$^{-1}$) and $M_1$ is the molecular weight of DETA (i.e., 103 g.mol$^{-1}$). The weights of the samples after the reaction were measured using a Sartorius BS 224S digital balance, which has a measurement resolution of 0.1 mg.

### 4.3.5 Adsorption Behavior

#### 4.3.5.1 Effects of pH and Contact Time

The APAN nanofiber mat specimens (i.e., 0.1 g each) were individually placed in a flask containing 20.0 mL solution of Cu(II), Ag(I), Pb(II), or Fe(II) ions. The initial concentration of the ions was 200 ppm. Each flask was shaken in a thermostatic shaker bath, operating at 30 °C and 100 rpm. To investigate the effect of pH, the initial pH of the testing solutions was adjusted between 2.0 to 7.0, using either 0.1 M HCl or 0.1 M NaOH aqueous solutions. To refrain the metal ions from precipitation, the pH of greater than 7.0 was not studied. To investigate the effect of contact time, the initial pH of the testing solutions was chosen from the

optimal pH value that resulted in high adsorption of the metal ions. In either case, 1 mL of each of the testing solutions was withdrawn (at 24 h, in the case of the effect of pH, and at an arbitrary time point, ranging from 0 to 24 h, in the case of the effect of contact time) and diluted with a proper amount of distilled water (i.e., sample solution). The sample solutions were then quantified for the amounts of metal ions by a Varian SpectrAA-300 atomic absorption spectroscope (AAS).

The amount of the metal ions adsorbed onto each fiber mat specimen [i.e., the adsorption capacity ($q$), in $mg \cdot g^{-1}$] was calculated based on the following equation [28]:

$$q = \frac{(C_0 - C_e)V}{M}, \qquad (2)$$

where $C_0$ and $C_e$ are the initial and the equilibrium concentrations of the metal ions in the testing solution ($mg \cdot L^{-1}$), $V$ is the volume of the testing solution (L), and $M$ is the weight of the adsorbent (i.e., 0.1 g).

### 4.3.5.2 Adsorption Isotherms

The adsorption isotherm of each type of the metal ions on the APAN nanofiber mats was studied by placing nanofiber mat specimens (0.1 g each) in a series of flasks containing 20.0 mL solutions of Cu(II), Ag(I), Pb(II), or Fe(II) ions of varying initial concentrations, ranging from 40 to 1000 ppm. The initial pH of the testing solutions was the same as that used in the experiment for studying the effect of the contact time. The flasks were each equilibrated in the shaker bath, operating at 30 °C and 100 rpm. After the 24 h contacting period, 1 mL of each of the testing solutions was withdrawn, diluted with a proper amount of distilled water, and quantified for the amount of metal ions by AAS. Equation (2) was used to calculate the adsorption capacities of the obtained data.

### 4.3.6 Desorption of Metal Ions from The APAN Nanofiber Mat

When adsorption equilibrium was reached, the fiber mats were rinsed with distilled water to remove any residual solution and were then dried *in vacuo* at room temperature (25 ± 1 °C). The desorption of metal ions was carried out by using HCl aqueous solutions of varying concentrations. The contents of the flasks were

shaken at 100 rpm and 30 °C for 1 h. The ion concentrations in the solutions were analyzed by AAS. The desorption ratio (D, in %) was calculated as follows [36]:

$$D\% = \frac{(mg\ of\ metal\ ion\ desorbed \times 100)}{mg\ of\ metal\ ion\ adsorbed\ onto\ fiber\ mats}, \qquad (3)$$

## 4.4 Results and Discussions

### 4.4.1 Characterization of APAN Nanofiber Mats

Morphologies of the neat and the aminated PAN nanofiber mats were observed by SEM and the results are shown in Figure 1. Evidently, the cross-sections of the neat PAN fibers were round and their surfaces were smooth. The diameters of these fibers were rather uniform, with the values being 192 ± 55 nm. The size of these fibers was comparable to that reported by Sutasinpromprae et al. [29]. Reacting the neat PAN fibers with DETA for 1 h caused the obtained APAN fibers to be more intertwined without expressing a strong influence on their overall morphology, as the cross-sections of the majority of the fibers were still round and their surfaces were still smooth. Nevertheless, there was evidence of adjacent fiber segments fusing to each other at touching points. Increasing the reaction time up to 4 h only caused the obtained APAN fibers to become more intertwined and the occurrence of fiber segments fusing to each other at touching points was more frequent. The diameters of the APAN electrospun fibers that had been reacted for 1, 2, 3, and 4 h were 194 ± 50, 198 ± 60, 186 ± 60, and 196 ± 60 nm, respectively. Clearly, the size of the obtained fibers was essentially similar to that of the neat PAN fibers. For the PAN nanofiber mats that had been reacted for 5 h, the conglutination of adjacent fibers was so severe that the materials started to lose their individually fibrous character. Moreover, the size of these fibers increased sharply to 231 ± 75 nm. Due to the considerable change to the morphology of the obtained APAN electrospun fibers, the reaction time of 5 h was not considered further. Since 4 h was the longest reaction time that did not result in the noticeable change in the morphology of the fibers, it was chosen to prepare the APAN nanofiber mat for further studies.

The FT-IR spectra of the neat and the aminated PAN nanofiber mats are shown in Figure 2. The spectrum of the neat PAN fiber mat exhibited adsorption peaks at 2242 and 1731cm$^{-1}$, corresponding to the stretching vibrations of the nitrile group and the carbonyl group of the ester of the methylacrylate co-monomer [28], respectively. The spectra of the APAN fiber mats, on the other hand, showed new absorption bands at 3346, 1650, 1600, 1573, and 1479 cm$^{-1}$. These can be assigned to the streching vibrations of the secondary amine (N–H), the amidine group (N–C=N) and the primary amine (NH$_2$) and the bending vibrations of the secondary amine and the methyl group of DETA, respectively [22, 24]. The intensities of these peaks increased with an increase in the reaction time. The peak of the carbonyl ester, on the other hand, was reduced in its intensity, indicating the disappearance of the methylacrylate group from the surface of the PAN nanofibers upon reacting with DETA [22, 24]. The peak associated with the nitrile group of the APAN nanofiber mats at 2242 cm$^{-1}$ decreased in its intensity as the reaction time, hence the conversion, increased (Table 4.1). Moreover, the reason for the conversion value of the APAN nanofiber mat which was greater than that of the corresponding APAN microfibers (Table 4.1) should be a direct result of the specific surface area of the electrospun PAN fiber mat that was greater than that of the PAN microfibers. Based on the FT-IR results, the mechanism of the reaction between PAN and DETA could be proposed as Scheme 4.1.

### 4.4.2 Adsorption Behavior

#### 4.4.2.1 Effect of pH

The adsorption of metal ions on the surface of the APAN nanofiber mats that had been prepared at the reaction time of 4 h was studied and the results are shown as a function of the initial pH of the testing solutions in Figure 4.3. At the lowest initial pH investigated, small amounts of metal ions could be adsorbed onto the materials, due particularly to the competitive adsorption between the prevalently-available H$^+$ and the metal ions. Moreover, the positive charges as resulting from the protonation of the primary and the secondary amines of the DETA ligands gave a strong electrostatic repulsive force to the positively-charged metal ions [27]. The amounts of the metal ions adsorbed onto the APAN nanofibers increased significantly with an increase in the initial pH of the testing solutions. As

the amounts of the protons decreased, the number of the protonated amine groups also decreased. As a result, more amine groups are available to capture the metal ions (i.e., via the interaction of the metal ions with the lone-pair electrons of nitrogen) [13]. Further increase in the initial pH of the testing solutions resulted in the amounts of the adsorbed metal ions reaching plateau values, and, in most cases [except for the adsorption of Ag(I) ions], the amounts of the adsorbed metal ions decreased as the initial pH approached the neutrality [25, 37-39]. This could be due to the competitive adsorption from the OH⁻ ions via the formation of the hydrogen bonding, resulting in the reduction of the adsorptive sites on the surface of the APAN nanofibers. Moreover, at these pH levels, the concentration of OH⁻ ions is high enough to interact with the metal ions, reducing the availability of the metal ions in their free, hydrated form to interact with the amine groups of the DETA ligands.

At the initial concentration of the metal ions in the testing solutions of 200 ppm, the optimal, initial pH level was found to be 4.0, as 90.5, 99.9, 100, and 97.0% of Cu(II), Ag(I), Fe(II), and Pb(II) ions could be removed from the testing solutions. Consequently, the initial pH of 4.0 was chosen for subsequent studies.

### 4.4.2.2 Effect of Contact Time

Figure 4.4 shows the effect of the contact time on the adsorption capacity of the APAN nanofiber mats, the APAN microfibers, and the as-received PAN microfibers for Cu(II), Ag(I), Fe(II), and Pb(II) ions. The adsorption of all of the four metal ions on the PAN microfibers was low, with the maximal values being at about 20%. This should be a result of the weak interaction between the metal ions and the lone-pair nitrogen electrons of the nitrile group on the surface of the fibers [25]. For the APAN nanofiber mats and the APAN microfibers, considerably greater amounts of metal ions could be adsorbed on these materials, a direct result of the introduction of the acryloamidino diethylenediamine group on their surfaces [21-24, 27]. Clearly, the adsorption increased with an increase in the contact time and reached equilibria within 10 h for the Cu(II) ions and 5 h for the Ag(I), Fe(II), and Pb(II) ions. There are two steps in the adsorption of these metal ions. In the initial step, adsorption was swift because of the great number of free adsorptive sites and the high concentration of the metal ions. In the second step,

adsorption rates decreased and finally reached equilibria. This was the direct effect from the depletion of the adsorptive sites as well as the decrease in the metal ion concentration in the testing solutions [10]. Comparatively, preferential adsorption of Cu(II) ions was observed on the APAN nanofiber mats, while both types of substrates exhibited similar adsorption towards the rest of the metal ions investigated. To ensure the equilibratory adsorption of the metal ions on the APAN nanofiber mats, the contact time of 24 h was chosen for subsequent studies.

### 4.4.2.3 Adsorption Isotherms

The effect of the initial concentration ($C_0$) of the metal ions in the testing solutions on the adsorption capacities of these ions onto the APAN nanofiber mats is shown in Figure 5. For each type of the metal ions, the adsorption capacity increased initially with increasing $C_0$ and reached a saturation point as $C_0$ increased further. Various mathematical models can be used to analyze adsorption data. The most common ones are the Langmuir and the Freundlich models [13, 40].

The Langmuir model was derived to describe the adsorption of an adsorbate on a homogenous, flat surface of an adsorbent and each adsorptive site can be only occupied once in a one-on-one manner. Mathematically, the model can be written as follows [27, 28]:

$$\frac{C_e}{q_e} = \frac{C_e}{q_m} + \frac{1}{K_L q_m},$$

(3)

where $C_e$ is the equilibrium concentration of metal ions in the testing solution (mg·L$^{-1}$), $q_e$ and $q_m$ are the equilibrium and the maximal adsorption capacities of the metal ions on the adsorbent (mg·g$^{-1}$), and $K_L$ is the adsorption equilibrium constant (L·mg$^{-1}$). The value of $q_m$ is taken as the slope of the plot of $C_e/q_e$ versus $C_e$, while that of $K_L$ can be calculated from the values of the slope and the $y$-intercept of the plot (i.e., slope/$y$-intercept). The values of these parameters, as analyzed from the plots shown in Figure 4.5, are summarized in Table 4.2.

Unlike the Langmuir model, the Freundlich model is used to describe the adsorption of an absorbate on a heterogeneous surface of an adsorbent. The mathematical expression of the model is given as follows [27]:

$$q_e = K_F C_e^{1/n} , \qquad (4)$$

where $K_F$ [$mg^{(1-1/n)} \cdot L^{1/n} \cdot g^{-1}$] and $n$ are Freundlich constants. By plotting $\log q_e$ as a function of $\log C_e$, the value of $K_F$ is taken as the anti-logarithmic value of the $y$-intercept and $n$ is the inverse value of the slope. The values of these parameters, which were also analyzed from the plots shown in Figure 4.5, are summarized in Table 4.2.

According to the obtained results, the adsorption data of the four metal ions on the APAN nanofiber mats were fitted particularly well with the Langmuir model, as indicated by the very high values of the correlation coefficient ($r^2$). As shown in Table 4.2, the maximal adsorption capacities of Cu(II), Ag(I), Fe(II), and Pb(II) ions on the APAN nanofiber mats were 150.6, 155.5, 116.5, and 60.6 $mg \cdot g^{-1}$, respectively, which was higher than APAN microfibers. This can be evaluate that the higher specific area can improve the adsorption behavior of the adsorbent.

### 4.4.2.4 Adsorption Kinetics

The results as obtained in the Section 3.2.2 were further analyzed to obtain the information on the adsorption kinetics of the four metal ions on the APAN nanofiber mats. The pseudo first order kinetic model is based on the approximation that the adsorption rate relates to the number of the unoccupied, adsorptive sites. The model, in its final form, can be written as follows [36, 41]:

$$\log(q_e - q_t) = \log q_e - \frac{k_1}{2.303} t, \qquad (5)$$

where $q_t$ is the adsorption capacity of the metal ions on an adsorbent at an arbitrary time $t$ ($mg \cdot g^{-1}$) and $k_1$ is the pseudo-first-order rate constant ($min^{-1}$). By plotting $\log(q_e - q_t)$ as a function of the contact time $t$, the values of the calculated $q_e$ (i.e., $q_{e,cal}$) and the rate constant $k_1$ can be obtained from the anti-logarithmic value of the $y$-intercept and the slope of the plot, respectively. The adsorption of Cu(II), Ag(I), Fe(II), and Pb(II) ions, at the initial concentration of 200

ppm, onto the APAN nanofiber mats, as shown in Figure 4.4, were analyzed. The results are graphically shown Figure 4.6, while the values of $k_1$ and $q_{e,cal}$ along with those of the correlation coefficient ($r^2$) are summarized in Table 4.3.

On the other hand, the adsorption rate could also be approximated based on the pseudo second order kinetic model. This model is derived based on the notion that the adsorption should relate to the squared product of the difference between the number of the equilibrium adsorptive sites available on an adsorbent and that of the occupied sites. The model, in its final form, can be expressed as follows [36, 41]:

$$\frac{t}{q_t} = \frac{1}{k_2 q_e^2} + \frac{t}{q_e},\tag{6}$$

where $k_2$ is the pseudo-second-order rate constant ($g \cdot mg^{-1} \cdot min^{-1}$). The analyses of the data, such as those shown in Figure 4, could be done through the construction of plots of $t/q_t$ as a function of the contact time $t$, as shown in Figure 7. Linear plots should be obtained, with the values of the calculated $q_e$ (i.e., $q_{e,cal}$) and the rate constant $k_2$ can be obtained from the inverse values of the slope and the $y$-interception values, respectively. The values of $k_2$ and $q_{e,cal}$ along with those of the correlation coefficient ($r^2$) are also summarized in Table 4.3.

Based on the values of the correlation coefficient ($r^2$), the experimental data were fitted better with the pseudo second order kinetic model than the pseudo first order kinetic model. Moreover, the $q_{e,cal}$ values as obtained from the pseudo second order kinetic model appeared to be very close to the experimentally-observed values than do the values from the pseudo first order kinetic model.

### 4.4.2.5 Desorption Characteristics

The effects of acidity of acid for Cu(II), Ag(I), Fe(II), and Pb(II) ion desorption from the APAN nanofiber mat were also studied. Desorption of the metal ions was conducted with 20 mL of 2 to 10 M hydrochloric acid. The results shown in Figures 4.8 confirm that these metal ions can be desorbed with 20 mL of a 10 M HCl solution from the APAN nanofiber mat, with a desorption efficiency

above 90 %. These results suggest that the APAN nanofiber mat may be a good adsorbent for heavy metal ions and may use in wastewater treatment efficiently.

## 4.5 Conclusions

The APAN nanofiber mats were obtained from the reaction between the electrospun PAN nanofiber mats and DETA. The conversion of the nitrile group, native to PAN, into the the amidino diethylenediamine group, native to APAN, increased with an increase in the reaction time. The chelating property of the obtained APAN nanofiber mats was evaluated against Cu(II), Ag(I), Fe(II), and Pb(II) ions. The initial pH of the testing solutions posed a strong influence on the adsorption behavior of the materials, with the initial pH of 4.0 being the optimal value where the APAN nanofiber mats showed high adsorption towards all four types of the metal ions. On the other hand, the adsorption capacity was found to increase with an increase in the contact time and the equilibria were reach at about 10 h for Cu(II) ions and about 5 h for the rest. The adsorption of these metal ions was fitted well with the Langmuir equation, with the maximal adsorption capacities were calculated to be 150.6, 155.5, 116.5, and 60.6 $mg \cdot g^{-1}$ for Cu(II), Ag(I), Fe(II), and Pb(II) ions, respectively. The transient adsorption data of the four metal ions on the APAN nanofiber mats were better described with the pseudo second order kinetic model. Lastly, the nanofiber mats (0.1 g) can be generated by using 20 mL of a 10 M HCl solution, with a desorption efficiency greater than 99 %. These results suggest that the APAN nanofiber mat may be a good adsorbent for heavy metal ions and may have great potential use in wastewater treatment.

## 4.6 Supplementary Data

Supplementary data associated with this research work can be found in the online version, at http://pubs.acs.org/doi/suppl/10.1021/ie200504c

## 4.7 Acknowledgements

## 4.7 References

[1]   Mahmoud, M.E.; Osman, M.M.; Hafez, O.F.; Elmelegy, E. Removal and preconcentration of lead (II), copper (II), chromium (III) and iron (III) from wastewaters by surface developed alumina adsorbents with immobilized 1-nitroso-2-naphthol, J. Hazard. Mater. 173 (2010) 349–357.

[2]   Shukla, S.R.; Pai, R.S.; Shendarkar, A.D. Adsorption of Ni(II), Zn(II) and Fe(II) on modified coir fibres, Sep. Purif. Technol. 47 (2006) 141–147.

[3]   Navarro, R.R.; Wada, S.; Tatsumi, K. Heavy metal precipitation by polycation–polyanion complex of PEI and its phosphonomethylated derivative, J. Hazard. Mater. B123 (2005) 203–209.

[4]   Panayotova, T.; Dimova-Todorova, M.; Dobrevsky, I. Purification and reuse of heavy metals containing wastewaters from electroplating plants, Desalination 206 (2007) 135–140.

[5]   Dąbrowski, A.; Hubicki, Z.; Podkościelny, P.; Robens, E. Selective removal of the heavy metal ions from waters and industrial wastewaters by ion-exchange method, Chemosphere 56 (2004) 91–106.

[6]   Mbareck, C.; Nguyen, Q.T.; Alaoui, O.T.; Barillier, D. Elaboration, characterization and application of polysulfone and polyacrylic acid blends as ultrafiltration membranes for removal of some heavy metals from water, J. Hazard. Mater. 171 (2009) 93–101.

[7]   O'Connell, D.W.; Birkinshaw, C.; O'Dwyer, T.F. Heavy metal adsorbents prepared from the modification of cellulose: A review, Bioresource Technol. 99 (2008) 6709–6724.

[8] Zhu, S.; Yang, N.; Zhang, D. Poly($N$,$N$-dimethylaminoethyl methacrylate) modification of activated carbon for copper ions removal, Mater. Chem. Phys. 113 (2009) 784–789.

[9] Zhang, S.; Li, X.; Chen, J.P. Preparation and evaluation of a magnetite-doped activated carbon fiber for enhanced arsenic removal, Carbon 48 (2010) 60–67.

[10] Mishra, P.C.; Patel, R.K. Removal of lead and zinc ions from water by low cost adsorbents, J. Hazard. Mater. 168 (2009) 319–325.

[11] Dragan, E.S.; Dinu, M.V.; Timpu, D. Preparation and characterization of novel composites based on chitosan and clinoptilolite with enhanced adsorption properties for $Cu^{2+}$, Bioresource Technol. 101 (2010) 812–817.

[12] Wang, X.; Zheng, Y.; Wang, A. Fast removal of copper ions from aqueous solution by chitosan-g-poly(acrylic acid)/attapulgite composites, J. Hazard. Mater. 168 (2009) 970–977.

[13] Shen, W.; Chen, S.; Shi, S.; Li, X.; Zhang, X.; Hu, W.; Wang, H. Adsorption of Cu(II) and Pb(II) onto diethylenetriamine-bacterial cellulose, Carbohyd. Polym. 75 (2009) 110–114.

[14] Jiang, Y.; Pang, H.; Liao, B. Removal of copper(II) ions from aqueous solution by modified bagasse, J. Hazard. Mater. 164 (2009) 1–9.

[15] Zhang, G.; Qu, R.; Sun, C.; Ji, C.; Chen, H.; Wang, C.; Niu, Y. Adsorption for Metal Ions of Chitosan Coated Cotton Fiber, J. Appl. Polym. Sci.110 (2008) 2321–2327.

[16] Sun, S.; Wang, A. Adsorption properties of N-succinyl-chitosan and cross-linked N-succinyl-chitosan resin with Pb (II) as template ions, Sep. Purif. Technol. 51 (2006) 409–415.

[17] Kavaklı, P.A.; Güven, O. Removal of Concentrated Heavy Metal Ions from Aqueous Solutions Using Polymers with Enriched Amidoxime Groups, J. Appl. Polym. Sci. 93 (2004) 1705–1710.

[18] Bilba, N.; Bilba, D.; Moroi, G. Synthesis of a Polyacrylamidoxime Chelating Fiber and Its Efficiency in the Retention of Palladium Ions, J. Appl. Polym. Sci. 92 (2004) 3730–3735.

[19] Gong, B. Synthesis of polyacrylaminoimidazole chelating fiber and properties of concentration and separation of trace Au, Hg and Pd from samples, Talanta 57 (2002) 89–95.

[20] Chang, X.; Su, Q.; Liang, D.; Wei, X.; Wang, B. Efficiency and application of poly(acryldinitrophenylamidrazone-dinitroacrylphenylhydrazine) chelating fiber for pre-concentrating and separating trace Au(III), Ru(III), In(III), Bi(III), Zr(IV), V(V), Ga(III) and Ti(IV) from solution samples, Talanta 57 (2002) 253–261.

[21] Deng, S.; Bai, R. Removal of trivalent and hexavalent chromium with aminated polyacrylonitrile fibers: performance and mechanisms, Water Res. 38 (2004) 2424–2432.

[22] Deng, S.; Bai, R.; Chen, J.P. Aminated Polyacrylonitrile Fibers for Lead and Copper Removal, Langmuir 19 (2003) 5058–5064.

[23] Ma, N.; Yang, Y.; Chen, S.; Zhang, Q. Preparation of amine group-containing chelating fiber for thorough removal of mercury ions, J. Hazard. Mater. 171 (2009) 288–293.

[24] Ko, Y.G.; Choi, U.S.; Park, Y.S.; Woo, J.W. Fourier Transform Infrared Spectroscopy Study of the Effect of pH on Anion and Cation Adsorption onto Poly(acryloamidino diethylenediamine), J. Polym. Sci. Pol. Chem. 42 (2004) 2010–2018.

[25] Türkmen, D.; Yılmaz, E.; Öztürk, N.; Akgöl, V; Denizli, A. Poly(hydroxyethyl methacrylate) nanobeads containing imidazole groups for removal of Cu(II) ions, Mater. Sci. Eng. C 29 (2009) 2072–2078.

[26] Liu, X.; Hu, Q.; Fang, Z.; Zhang, X.; Zhang, B. Magnetic Chitosan Nanocomposites: A Useful Recyclable Tool for Heavy Metal Ion Removal, Langmuir 25 (2009) 3-8.

[27] Huang, S.; Chen, D. Rapid removal of heavy metal cations and anions from aqueous solutions by an amino-functionalized magnetic nano-adsorbent, J. Hazard. Mater. 163 (2009) 174–179.

[28] Saeed, K.; Haidera, S.; Oh, T.J.; Park, S.Y. Preparation of amidoxime-modified polyacrylonitrile (PAN-oxime) nanofibers and their applications to metal ions adsorption, J. Membrane Sci. 322 (2008) 400–405.

[29] Sutasinpromprae, J.; Jitjaicham, S.; Nithitanakul, M.; Meechaisue, C.; Supaphol, P. Preparation and characterization of ultrafine electrospun polyacrylonitrile fibers and their subsequent pyrolysis to carbon fibers, Polym Int. 55 (2006) 825–833.

[30] Reneker, D.H.; Yarin, A. L. Electrospinning jets and polymer nanofibers, Polymer 49 (2008) 2387-2425.

[31] Shin, Y. M.; Hohman, M.M; Brenner, M.P.; Rutledge, G.C. Experimental characterization of electrospinning: the electrically forced jet and instabilities, Polymer 42 (2001) 9955-9967.

[32] Ding, B.; Kim, H.Y.; Lee, S.C.; Shao, C.L.; Lee, D.R.; Park, S.J.; Kwag, G.B.; Choi, K.J. Preparation and characterization of a nanoscale poly(vinyl alcohol) fiber aggregate produced by an electrospinning method, J. Polym. Sci. Pol. Phys. 40 (2002) 1261-1268.

[33] Wu, L.L.; Yuan, X.Y.; Sheng, J. Immobilization of cellulase in nanofibrous PVA membranes by electrospinning, J. Membrane Sci. 250 (2005) 167-173.

[34] Luu, Y.K.; Kim, K.; Hsiao, B.S.; Chu, B.; Hadjiargyrou, M. Development of a nanostructured DNA delivery scaffold via electrospinning of PLGA and PLA-PEG block copolymers, J. Control Release 89 (2003) 341-353.

[35] Kenawy, E.R.; Bowlin, G.L.; Mansfield, K.; Layman, J.; Simpson, D.G.; Sanders, E.H.; Wnek, G.E. Release of tetracycline hydrochloride from electrospun poly(ethylene-co-vinylacetate), poly(lactic acid), and a blend, J. Control Release. 81 (2002) 57-64.

[36] Chen, C.; Lin, M.; Hsu, K. Recovery of Cu(II) and Cd(II) by a chelating resin containing aspartate groups, J. Hazard. Mater. 152 (2008) 986–993.

[37] Kyzas, G.Z.; Kostoglou, M.; Lazaridis, N.K. Copper and chromium(VI) removal by chitosan derivatives—Equilibrium and kinetic studies, Chem. Eng. J. 152 (2009) 440–448.

[38] Jing, X.; Liu, F.; Yang, X.; Ling, P.; Li, L.; Long, C.; Li, A. Adsorption performances and mechanisms of the newly synthesized N,N_-di(carboxymethyl) dithiocarbamate chelating resin toward divalent heavy metal ions from aqueous media, J. Hazard. Mater. 167 (2009) 589–596.

[39] Kara, A.; Uzun, L.; Beşirli, N.; Denizli, A. Poly(ethylene glycol dimethacrylate-*n*-vinyl imidazole) beads for heavy metal removal, J. Hazard. Mater. 106B (2004) 93–99.

[40] Dinu, M.V.; Dragan, E.S. Heavy metals adsorption on some iminodiacetate chelating resins as a function of the adsorption parameters, React. Funct. Polym. 68 (2008) 1346–1354.

[41] Monier, M.; Ayad, D.M.; Sarhan A.A. Adsorption of Cu(II), Hg(II), and Ni(II) ions by modified natural wool chelating fibers, J. Hazard. Mater. 176 (2009) 348-355.
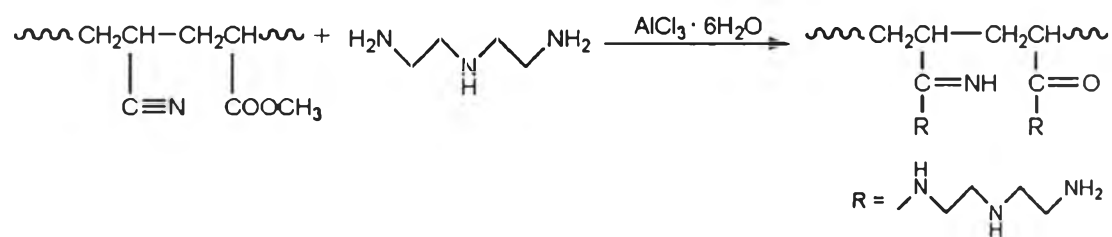
**Scheme 4.1** Chemical reaction between PAN and DETA.

Table 4.1 Conversion ($C_n$ , in %) of the nitrile group of the neat electrospun PAN nanofibers and the as-received PAN microfibers into the amidino diethylenediamine group of the corresponding APAN fibers at different reaction times ($n$ = 5).

| Sample type | Electrospun PAN nanofibers | | | | As-received PAN microfibers |
|---|---|---|---|---|---|
| Reaction time (h) | 1 | 2 | 3 | 4 | 4 |
| % Conversion | 13.4 ± 1.3 | 18.3 ± 1.3 | 45.7 ± 1.42 | 58.5 ± 2.4 | 31.6 ± 2.9 |

Table 4.2 Values of the parameters associated with the Langmuir and the Freundlich models, including those of the correlation coefficient, for the adsorption of Cu(II), Ag(I), Fe(II), and Pb(II) ions on the APAN nanofiber mats.

| Metal ions | Langmuir model | | | Freundlich model | | |
|---|---|---|---|---|---|---|
| | $q_m$ (mg·g$^{-1}$) | $K_L$ (L·mg$^{-1}$) | $r^2$ | $K_F$ [mg$^{(1-1/n)}$·L$^{1/n}$·g$^{-1}$] | $n$ | $r^2$ |
| Cu(II) | 150.6 | 0.013 | 0.9923 | 13.43 | 2.66 | 0.9644 |
| Ag(I) | 155.5 | 0.216 | 0.9989 | 50.82 | 5.03 | 0.9379 |
| Fe(II) | 116.5 | 0.613 | 0.9999 | 31.92 | 2.80 | 0.9813 |
| Pb(II) | 60.6 | 0.342 | 1.0000 | 22.13 | 3.43 | 0.9663 |

Table 4.3 Kinetics parameters describing the adsorption of Cu(II), Ag(I), Fe(II), and Pb(II) ions onto the APAN nanofiber mats (cf. results in Figure 4) based on the pseudo first- and the pseudo second order kinetic models.

| Metal ions | $q_{e,exp}$ (mg·g$^{-1}$) | Pseudo first order | | | Pseudo second order | | |
|---|---|---|---|---|---|---|---|
| | | $k_1$ (min$^{-1}$) | $q_{e,cal}$ (mg·g$^{-1}$) | $r^2$ | $k_2$ (min$^{-1}$) | $q_{e,cal}$ (mg·g$^{-1}$) | $r^2$ |
| Cu(II) | 29.62 | $5.67 \times 10^{-3}$ | 25.23 | 0.9944 | $4.29 \times 10^{-4}$ | 31.40 | 0.9987 |
| Ag(I) | 33.51 | $2.60 \times 10^{-2}$ | 29.99 | 0.9975 | $2.18 \times 10^{-3}$ | 33.97 | 0.9998 |
| Fe(II) | 33.20 | $3.20 \times 10^{-2}$ | 34.04 | 0.9809 | $1.90 \times 10^{-3}$ | 33.70 | 0.9997 |
| Pb(II) | 30.58 | $1.48 \times 10^{-2}$ | 31.62 | 0.9704 | $7.46 \times 10^{-4}$ | 31.72 | 0.9989 |
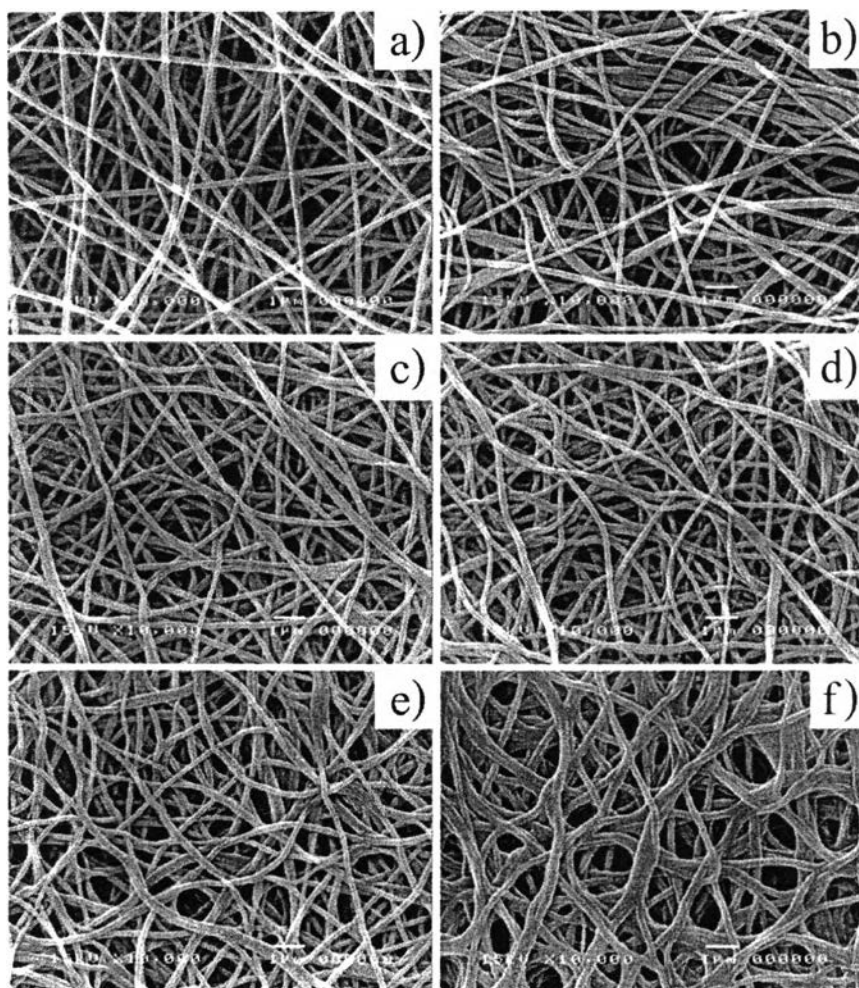
**Figure 4.1** Representative SEM images of (a) the neat electrospun PAN fiber mat and the APAN electrospun fiber mats that had been obtained from the reaction between the neat PAN electrospun fiber mat and DETA in the presence of AlCl$_3$·6H$_2$O at 90 °C for (b) 1, (c) 2, (d) 3, (e) 4, and (f) 5 h.
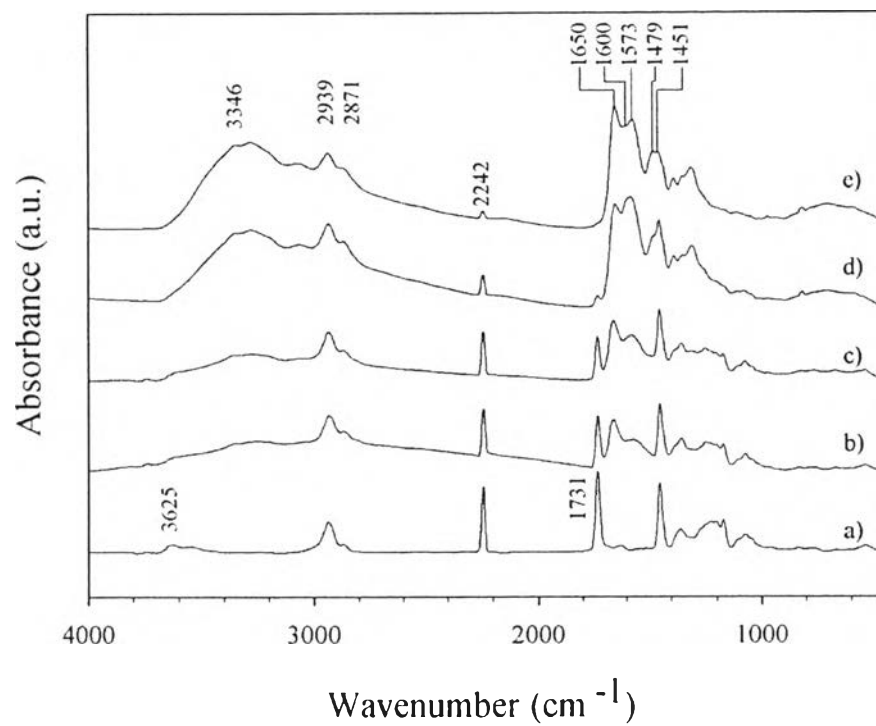
**Figure 4.2** FT-IR spectra of (a) the neat electrospun PAN fiber mat and the APAN electrospun fiber mats that had been obtained from the reaction between the neat PAN electrospun fiber mat and DETA in the presence of $AlCl_3 \cdot 6H_2O$ at 90 °C for (b) 1, (c) 2, (d) 3, and (e) 4 h.
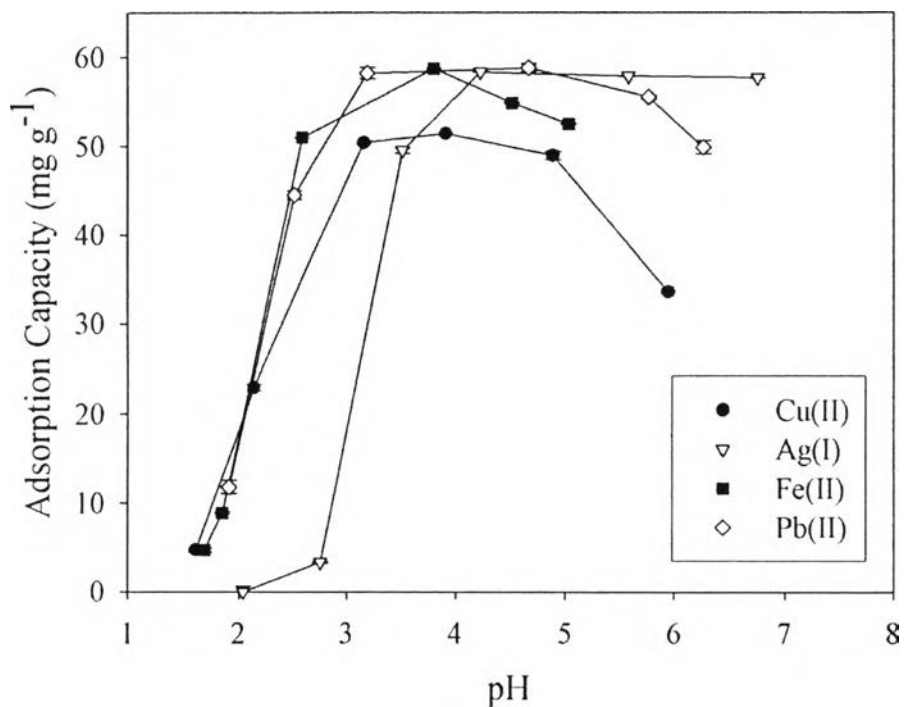
**Figure 4.3** Effect of the initial pH of the testing solutions on the adsorption of Cu(II), Ag(I), Fe(II), and Pb(II) ions onto the APAN nanofiber mats ($n$ = 5). Experimental condition: initial ion concentration = 200 ppm, sample dose = 0.1 g/20 mL, temperature = 30 °C, and contact time = 24 h.
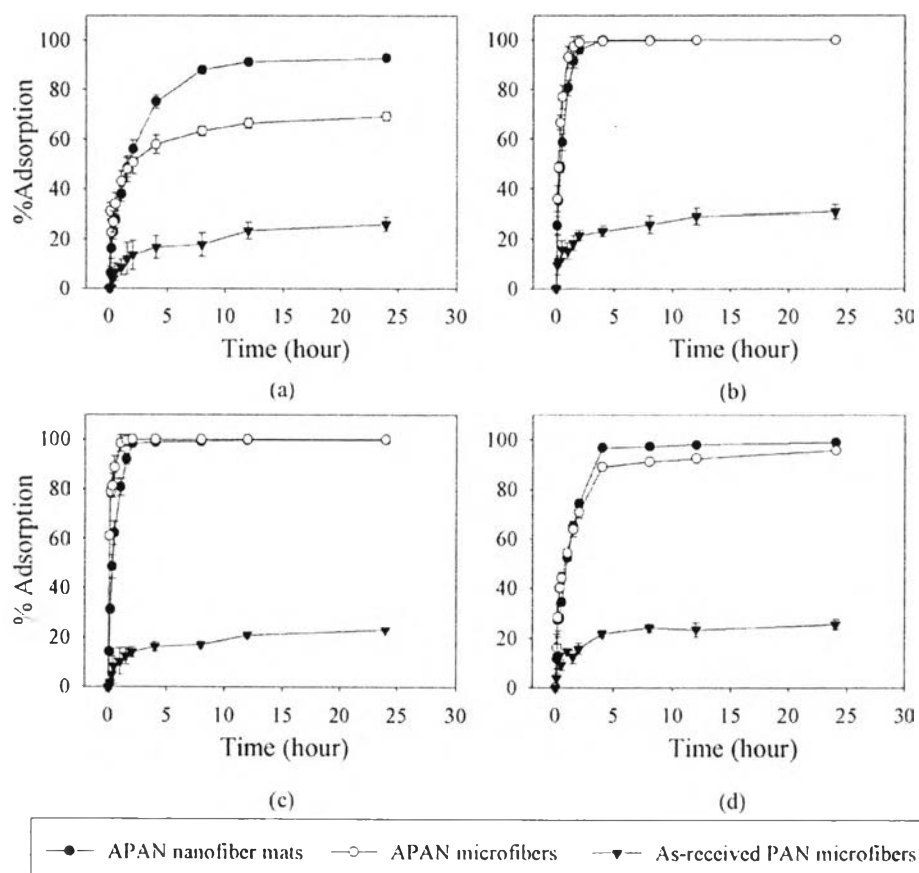
Figure 4.4 Effect of contact time on the adsorption of (a) Cu(II), (b) Ag(I), (c) Fe(II), and (d) Pb(II) ions onto the APAN nanofiber mats, the APAN microfibers, and the as-received PAN microfibers ($n$ = 5). Experimental condition: initial ion concentration = 200 ppm, sample dose = 0.1 g/20 mL, initial pH = 4.0, and temperature = 30 °C.
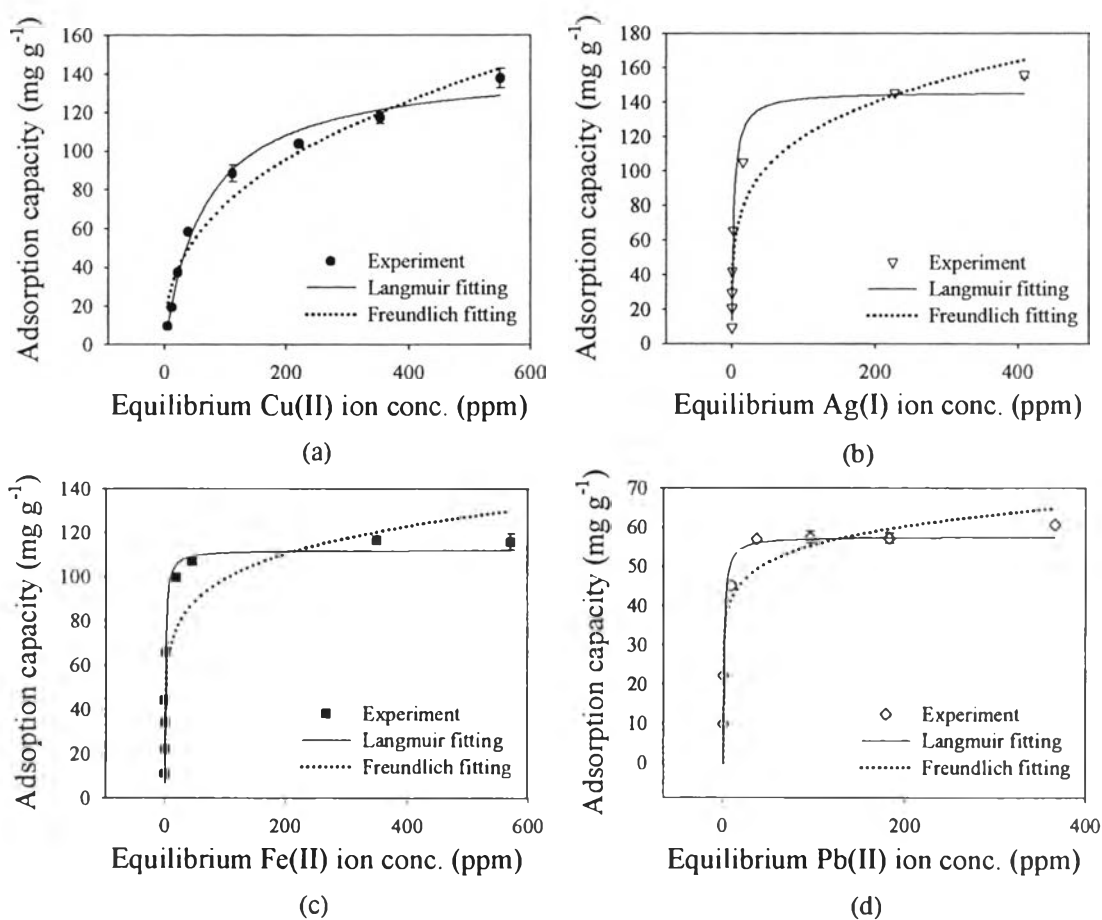
**Figure 4.5** Adsorption isotherms of Cu(II), Ag(I), Fe(II) and Pb(II) ions onto the APAN nanofiber mats ($n = 5$). Experimental condition: initial ion concentration = 40–1000 ppm, sample dose = 0.1 g/20 mL, initial pH = 4, temperature = 30 °C, and contact time = 24 h.
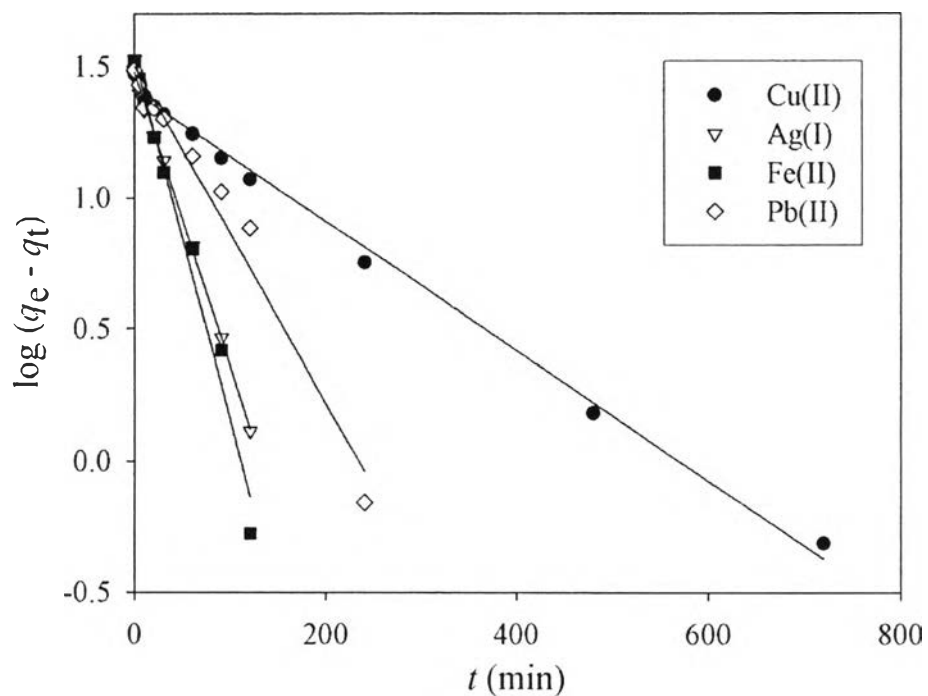
**Figure 4.6** Adsorption kinetics of Cu(II), Ag(I), Fe(II), and Pb(II) ions onto the APAN nanofiber mats (cf. results in Figure 4), based on the pseudo first order kinetic model.
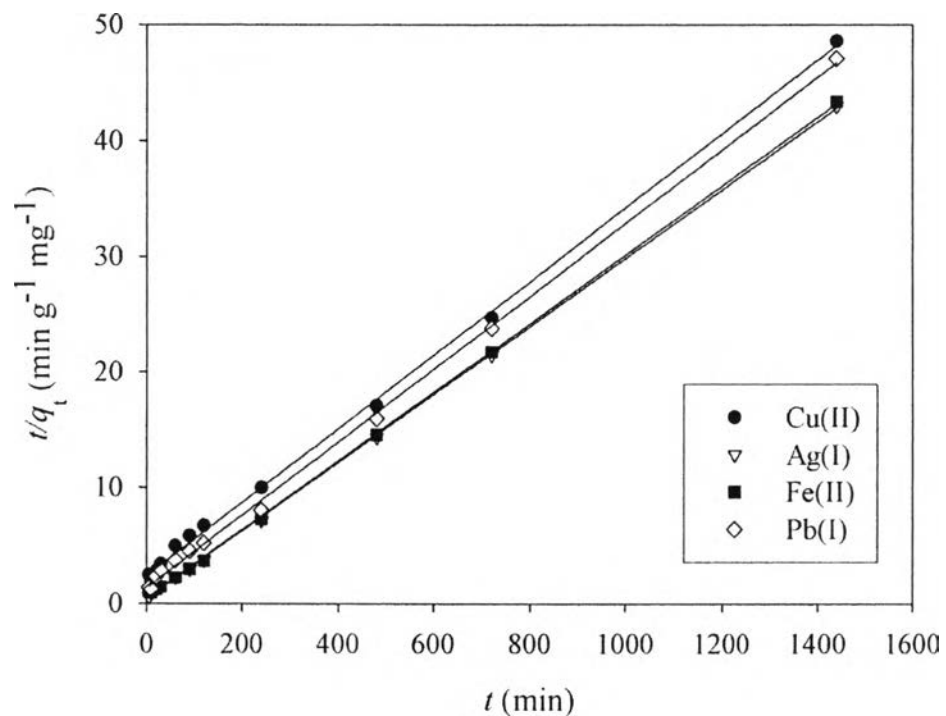
**Figure 4.7** Adsorption kinetics of Cu(II), Ag(I), Fe(II), and Pb(II) ions onto the APAN nanofiber mats (cf. results in Figure 4), based on the pseudo second order kinetic model.